Article

Not peer-reviewed version

Dermatological Application of *Pelargonium graveolens* Flower: A Novel Potential Source of Melanin Synthesis-Inhibiting Effects

Najlae El-otmani *, Mohamed Chebaibi , Ahmed Zahidi

Posted Date: 18 April 2025

doi: 10.20944/preprints202504.1496.v1

Keywords: *Pelargonium graveolens*; collagenase; Formulation; Pigmentation; Interfacial tension; Phytochemical analysis; in silico

 doi:10.20944/preprints202504.1496.v1

Article

Dermatological Application of *Pelargonium graveolens* Flower: A Novel Potential Source of Melanin Synthesis-Inhibiting Effects

Najlae El-otmani [1,2,*], Mohamed Chebaibi [3,4] and Ahmed Zahidi [1]

[1] Therapeutic Chemistry Laboratory, Department of Drug Sciences, Faculty of Medicine, and Pharmacy, Mohammed V University in Rabat, Morocco
[2] Department of Pharmaceutical Sciences, University of Basel, Klingelbergstrasse 50, 4056 Basel, Switzerland
[3] Higher Institute of Nursing Professions and Health Techniques, Fez, Morocco
[4] Biomedical and Translational Research Laboratory, Faculty of Medicine and Pharmacy of Fez, Sidi Mohamed Ben Abdellah University, Fez 30000, Morocco
* Correspondence: najlae.elotmani@unibas.ch or najlae.elotmani@um5r.ac.ma; Tel.: +417-834-061-85

Abstract: The increasing prevalence of skin-aging and pigmentation disorders, along with inflammation-related pathologies, has driven the search for novel enzyme inhibitors with targeted action against key enzymes such as elastase, collagenase, and tyrosinase. In this context, extracts from *Pelargonium graveolens* (*P. graveolens*) flowers were subjected to in vitro and in silico assays to evaluate their inhibitory effects on theses enzymes, as well as the BSA protein denaturation. Additional assessments of emulsification and photoprotective properties were conducted. The hydroethanolic sonication extract demonstrated potent therapeutic potential, with low IC_{50} values for BSA denaturation (0.31 ± 0.26 mg/mL), tyrosinase (0.06 ± 0.04 mg/mL), elastase (1.29 ± 0.58 mg/mL), and collagenase (0.28 ± 0.14 mg/mL). All extracts effectively reduced surface and interfacial tension, highlighting their potential as natural co-emulsifier. HPLC-PDA-MS/MS analysis identified key bioactive compounds, including shikimic acid, gallic acid diglucoside, and salvianolic acid M. In fact, Binding site prediction revealed that shikimic acid and dihydroxybenzoic acid from *P. graveolens* extract are likely the key compounds responsible for the inhibitory effects on elastase, collagenase, and tyrosinase. Additionally, trigallic acid appears to play a major role in the inhibition of BSA denaturation. Stability tests of novel formulations-based 2% *P. graveolens* supporting their potential for commercial applications.

Keywords: *Pelargonium graveolens*; collagenase; Formulation; Pigmentation; Interfacial tension; Phytochemical analysis; in silico

1. Introduction

The skin, as a complex organ enveloping the entire body, plays an essential role in defending the organism against extreme environmental conditions and infectious threats. Yet despite its protective functions, the skin is subject to various physiological and morphological deteriorations [1]. Conditions such as premature skin aging, hyperpigmentation and other skin afflictions, are reported by many patients to be uncomfortable, requiring a solution to reduce the degree of pigmentation, and improve overall skin tone [2]. Inflammatory skin conditions promote the generation of elevated melanin levels, affecting melanocytes; the responsible cells for pigment production on the skin [3]. This suggests that reducing inflammation in cells could help to reduce the risk of pigmentation. The tyrosinase enzyme is another target to control melanin production [4].

Recently, medicinal plant extracts are increasingly utilized in various commercial dermatological products for their protective, and anti-pigmentation properties [5–8]. Therefore, patients are more attracted by formulations containing herbal extracts than the synthetic ones [9]. For instance, *Pelargonium graveolens* (*P. graveolens*), commonly known as geranium, is highly regarded in

 doi:10.20944/preprints202504.1496.v1

cosmetics, and dermatology for its antioxidant, anti-tyrosinase, and antimicrobial properties. Traditionally, *P. graveolens* has been used to treat haemorrhoids, dysentery, inflammation and cancer [10,11]. However, progress in dermatological and cosmetic applications of this plant remains limited [12].

The present study examines the in vitro and in silico dermatological and Cosmeceutical potential of *P. graveolens* extracts. The optimum extract was then chemically profiled by HPLC-PDA-MS/MS, and the stability of novel formulations was monitored during 90 days for potential commercial application.

2. Materials and Methods

2.1. Plant Material and Extraction

P. graveolens; identified under the voucher code RAB114770, was harvested from Sahel Boutaher, situated in the Taounate region of Northwest Morocco, with coordinates at 34°29'052.067'' N and -4°48'17.397'' W. The flowers were manually collected in May 2022, then deposited in a sample library until drying at ambient temperature for two weeks. The dried flowers were crushed with an electric grinder (Fritsch, Industriestrasse 8 55743 Idar-Oberstein Germany.) until a fine powder was obtained (diameter ≤ 300 µm). Three extraction methods were then used to obtain the phytochemical compounds from the plant material: maceration (w/v: 10 g/100 ml), sonication (w/v: 10 g/100 ml) and infusion (w/v: 2.5 g/75 ml). The solvent used for maceration and sonication was ethanol (100%) and ethanol-water (70:30), while water (100%) was used for infusion.

2.2. Bovine Serum Albumin (BSA) Denaturation

The in vitro anti-inflammatory activity was assessed according to a method based on the denaturation of bovine serum albumin (BSA) as previously reported by Lekouaghet et al [13]. Briefly, the extract or standard (diclofenac, 50 mg) was combined with BSA solution (0.2%) in Tris buffer (pH 6.8), and the mixture was incubated at 37°C for 15 minutes followed by immersion in a 72°C water bath for 5 minutes. Protein precipitation was evaluated at 660 nm (RoHS Uv-1800pc, Macy, China) and results were expressed in CI50 (mg/mL). The negative control sample consisted of 0.5 ml of water and 0.5 ml of BSA solution and the diclofenac 50mg was used as a positive control. The blank sample contained 0.5 ml of extract and 0.5 ml of Tris buffer solution (pH 6.8).

2.3. Enzyme Inhibitory Activities

2.3.1. Tyrosinase

The tyrosinase enzyme inhibition using 3,4-dihydroxyphénylalanine (L-DOPA) as substrate, was used to evaluate the anti-pigmentation activity of P. graveolens flower extracts, in accordance with Al-Mijalli et al [14]. Briefly, 50 µL of the extract and 50 µL of fungal tyrosinase (330 U/mL, in 50 mM phosphate buffer, pH 6.5) were mixed after incubating at 37°C for 10 minutes. Subsequently, 500 µL of 5 mM L-DOPA solution was added to the reaction mixture, followed by incubation at room temperature in the dark for 30 minutes. Measurements were taken at 510 nm and kojic acid served as the positive control. Results were expressed as IC50 (mg/mL), and the inhibition percentage (I%) was calculated using the equation (2).

$$I\% = \frac{(A_{Control} - A_{Simple})}{A_{Control}} \times 100 \quad (1)$$

2.3.2. Elastase

Elastase inhibition assay was conducted according to the method described by Khatib et al [15]. Porcine pancreatic elastase enzyme was prepared at a stock concentration of 3.33 mg/mL in sterile water. The substrate N-Succinyl-Ala-Ala-Ala-p-nitroanilide (AAAPVN) was dissolved in 0.2 mM Tris–HCl buffer (pH = 8) to achieve a 1.6 mM solution. Next, 50 µL of the sample solution (ranging

 doi:10.20944/preprints202504.1496.v1

from 3 to 0.046 mg/mL), along with Tris–HCl buffer and enzyme, were pre-incubated for 15 minutes. Then, 50 µL of the substrate was added to reach a final volume of 200 µL, and the reaction mixtures were incubated for 20 minutes at 37°C. Absorbance was measured at 400 nm using a microplate reader (Fluostar Omega). Epigallocatechin gallate served as the positive control in the experiment, and the results were expressed as IC50 (mg/mL) and the percentage inhibition (I%) was calculated using the calculation formula (1).

2.3.3. Collagenase

Collagenase inhibition assay was adapted from the method of Kim et al [16]. The test was conducted in a Tricine buffer solution (pH 7.5) containing NaCl and CaCl2. Clostridium histolyticum collagenase enzyme (ChC-EC.3.4.23.3) was utilized at an initial concentration of 0.8 unit/mL, dissolved in the buffer, and N-[3-(2-furyl) acryloyl]-Leu-Gly-Pro-Ala (FALGPA) served as substrate. Extracts ranging from 4 to 0.25 mg/mL were incubated with the enzyme for 15 minutes at 37°C. The enzymatic reaction was initiated by adding the substrate, and absorbance was measured at 490 nm using a microplate reader. Epigallocatechin gallate was employed as a positive control, and the results were reported as IC50 (mg/mL) and the inhibition percentage (I%) was calculated using the equation (1).

2.4. UV-B Absorption: Photoprotective Effect

P. graveolens extracts were investigated for their protective activity against UV-B rays according to Mansur's method [17]. Briefly, the absorbance of the extracts (2 mg/ml) was measured at a range of wavelengths between 290 and 320 nm with 5 nm intervals using a UV-VIS spectrometer (RoHS Uv-1800pc, Macy, China). The Sun Protection Factor (SPF) was calculated by applying the equation (2), where EE x I values are constants as set by Sayre et al [41]. Zinc oxide was used as the positive control.

$$SPF = CF \times \sum_{290}^{320} EE(\lambda) \times (\lambda) \times Abs(\lambda) \quad (2)$$

where:

EE: Erythemogenic effect.
I: The radiation intensity.
Abs: Absorbance of extract.
CF: Correction factor.

2.5. Interfacial and Surface Tension Characteristics

Interfacial and surface tension were measured by the pendant drop method using a fully automatic tensiometer (DataPhysics Instruments GmbH - Filderstadt, Germany). Briefly, the extract (1%, w/w) was placed in glass syringe and injected through a 22-gauge stainless steel needle into air (surface tension), or soybean oil placed inside a glass cell (interfacial tension). The drop of extract solution was incubated for approximately 10 min inside the continuous phase, during which a high-resolution camera captured its dimensions to measure the interfacial or surface tension using the Young-Laplace equation and calculated automatically by dpiMAX software.

2.6. Phytochemical Analysis Using HPLC-PDA-MS/MS

Phytochemical analysis was conducted employing HPLC-PDA-MS/MS methodology. A SHIMADZU LC-MS 8050 system, comprising a triple quadruple spectrometer equipped with an ESI source, was employed. Separation was achieved using a C18 reversed-phase column (Zorbax Eclipse XDB-C18, rapid resolution, 4.6 × 150 mm, 3.5 µm, Agilent, Santa Clara, CA, USA). Gradient elution was carried out using water and acetonitrile (ACN) (both with 0.1% formic acid) from 5% to 90% ACN over 60 minutes at a flow rate of 1 mL/min. Sample injection was automated using the SIL-40C

 doi:10.20944/preprints202504.1496.v1

xs autosampler. LC solution software (Shimadzu, Japan) was utilized to control the instrument, and MS analysis was conducted in negative ion mode.

2.7. In silico Binding Site Prediction

2.7.1. Ligand

The phytochemicals detected in the plant extract via HPLC were sourced from the PubChem database in SDF format. Ligand optimization and preparation were conducted using the LigPrep module in Schrödinger-Maestro v11.5, with the OPLS3 force field applied. To account for possible ionization states, protonation adjustments were made within a pH range of 7.0 ± 2.0, and up to 32 stereoisomeric configurations were generated per compound [18,19].

2.7.2. Protein

Target proteins for the molecular docking study were retrieved from the Protein Data Bank (PDB, www.rcsb.org). The selected structures included Tyrosinase (PDB: 2Y9X), Collagenase (PDB: 2TCL), Elastase (PDB: 7EST), and BSA (PDB: 6QS9). Before docking, structural refinement steps were performed, including the addition of hydrogen atoms, correction of bond orders, elimination of water molecules, optimization of hydrogen-bonding networks, adjustment of receptor atom charges, and energy minimization using the OPLS3 force field [20,21].

2.7.3. Glide Standard Precision (SP) Ligand Docking

Molecular docking simulations were carried out using Glide's Standard Precision (SP) protocol within Schrödinger-Maestro v11.5. To improve docking accuracy, a penalty was imposed on amide bonds displaying non-physiological cis/trans configurations. Additionally, Van der Waals interactions were scaled to 0.80, and a partial charge cutoff was set at 0.15. The docking outcomes were evaluated based on glide scores, which indicate the binding affinity of each ligand after energy minimization. The ligand conformation with the most favorable (lowest) glide score was selected for further analysis [22,23].

2.8. Application on Aqueous Serum Formulas

2.8.1. Preparation

In a beaker of 1L, water, glycerin, and propylene glycol were mixed, followed by the introduction of the emulsifier and all other ingredients listed in Table 1. The mixture was then homogenized with a mechanical stirrer (Philips GmbH HR2535/00 650W, Hamburg, Germany). The solution was agitated until a uniform white aqueous mixture was obtained (approx. 3 minutes), cooled and collected in glass jars. The formula was also pH-adjusted with triethanolamine. Xanthan gum, tragacanth gum or Linum usitatissimum seed extract was used to provide a thicker consistency.

Table 1. Composition of the liquid serum formulas.

F1 (INCI)	%, w/w	F2 (INCI)	%, w/w	F3 (INCI)	%, w/w
Aqua	71.5	AQUA	71.5	AQUA	71.5
Xhantan gum	0.2	Tragacanth Gum	0.2	Linum usitatissimum seed extract	0.2
Sodium Benzoate	0.3	Sodium Benzoate	0.3	Sodium Benzoate	0.3
Glycerin	7	Glycerin	7	Glycerin	7

 doi:10.20944/preprints202504.1496.v1

Propylene glycol	4	Propylene glycol	4	Propylene glycol	4
Myritol	10	Myritol	6,5	Myritol	0.2
Polysorbate 80	0.5	Polysorbate 80	0.5	Carboxymethy cellulose	0.5
Triethanolamine (50%)	Q. s	Triethanolamine (50%)	Q. s	Triethanolamine (50%)	Q. s
P.graveolens extract	Q. s	*P.graveolens* extract	Q. s	*P. graveolens* extract	Q. s

Q. s: Quantum Satis.

2.8.2. Stability

PH, conductivity, water activity, and lipid oxidation stability were evaluated at various intervals post-production (1, 15, 30, 60, and 90 days) to detect any changes over time. pH and conductivity were measured directly from the samples using a pH and conductivity meter (BOECO Bench-CT-676, Germany). Water activity was assessed by measuring the weight difference of initial and dried sample at 100°C for 48 hours. Lipid oxidation was evaluated using (CDR FoodLab® Junior, Perugia, Italy) and results were expressed quantitatively as meqO2/Kg.

Physical stability was examined through centrifugation (Sigma 2-16P, Osterode am Harz, Germany) at 3000 rpm for 30 minutes, simulating accelerated conditions. Heating and freeze-thaw stability was evaluated by subjecting the samples to four cycles of 24 hours each, oscillating between freezing (1-7 °C), ambient temperature (20-25 °C), heating (39.5-40.5 °C), and back to ambient temperature [24].

2.9. Data analysis

Experiments were carried out in triplicate. Analysis of data was performed using Microsoft Excel, with results presented as mean ± standard deviation (SD). An ANOVA test followed by a Tukey's multiple comparisons test were undertaken using OriginPro 2024. Different results were considered significantly different at $p < 0.05$.

3. Results and Discussion

3.1. BSA Denaturation Assay

The in vitro anti-inflammatory activity of *P. graveolens* flower extracts using the bovine serum albumin (BSA) denaturation method is quantified in terms of IC_{50} values, as delineated in Table 2. Values of 0.20 ± 0.031, 0.38 ± 0.022, 0.44 ± 0.024, 0.61 ± 0.030, to 1.64 ± 0.111 mg/mL, respectively for hydroethanolic sonication, ethanolic maceration, hydroethanolic maceration, ethanolic sonication, and infusion. Notably, all extracts, except for the infusion extract, exhibited IC_{50} values close to that of diclofenac (50 mg), a known anti-inflammatory agent inhibiting BSA denaturation (IC_{50} = 0.175 ± 0.010 mg/mL), with statistical significance ($p < 0.05$). Several polar polyphenols, such as quercetin, ellagic acid, caffeic acid and other flavonoids, have been studied for their ability to inhibit protein denaturation and reduce inflammation [25,26]. Previously, Martins et al [27] demonstrated significant anti-inflammatory effects of *P. graveolens* leaves harvested in Brazil, using the inflammatory mediator release method. They reported major inhibition of the inflammatory mediator mainly in the crude extract, the ethyl acetate fraction, and the residual fraction, at a concentration of 0.05 mg/mL.

 doi:10.20944/preprints202504.1496.v1

3.2. Enzyme Inhibitory Activities

Tyrosinase inhibitors derived from plant extracts are of high interest, in view of their low toxicity and biological availability [4]. The investigation into the inhibitory potential of *P. graveolens* flower extracts against tyrosinase, a key enzyme involved in melanin synthesis, was undertaken in vitro across various concentrations. This study sought to elucidate the capacity of these extracts to impede tyrosinase activity, thereby implicating their potential in mitigating hyperpigmentation. Remarkably, both hydroethanolic extracts obtained through sonication and maceration exhibited notable dose-dependent inhibition of tyrosinase enzyme activity, as illustrated in Figure 1 (a). At a concentration of 2 mg/mL, the hydroethanolic extract obtained via sonication showcased a significant inhibition of 70.152 ± 3.725%, closely followed by the hydroethanolic extract obtained through maceration, demonstrating inhibition percentages of 83.366 ± 5.327%. This efficacy is comparable to the standard anti-pigmentation agent kojic acid, which exhibited a maximum inhibition of 86.946± 1.507%. Conversely, the ethanolic extracts demonstrated comparatively lower inhibitory effects on tyrosinase activity.

Quantitative analysis further elucidated the inhibitory potential of these extracts, with IC_{50} values presented in Table 2. Notably, the hydroethanolic extract obtained through sonication displayed the lowest IC_{50} value of 0.06 ± 0.079 mg/mL, followed by the hydroethanolic maceration extract (0.15 ± 0.103 mg/mL), ethanolic maceration extract (0.37 ± 0.017 mg/mL), ethanolic sonication extract, and infusion extract, in ascending order. Comparison with the reference standard, kojic acid, revealed its relatively lower IC_{50} value of 0.071 ± 0.013 mg/mL. Statistically, no significant differences were discerned between kojic acid and the investigated extracts ($p > 0.05$), except the ethanolic sonication extract, implying comparable efficacy across most samples. Previous work by El Aanachi et al [28] highlighted a significant tyrosinase inhibitory effect of the methanolic extract, obtained from the leaves of *P. graveolens*, with a remarkable IC_{50} value of 0.02 mg/mL. These findings underscore the promising anti-pigmentation activity of *P. graveolens* flower extracts, thus contributing to the burgeoning body of literature advocating for the integration of natural plant extracts over synthetic alternatives in cosmetics and pharmaceutical products. Various natural tyrosinase inhibitors are used as skin depigmenting compounds. Phenolic compounds have been reported to be important tyrosinase inhibitors [29,30].

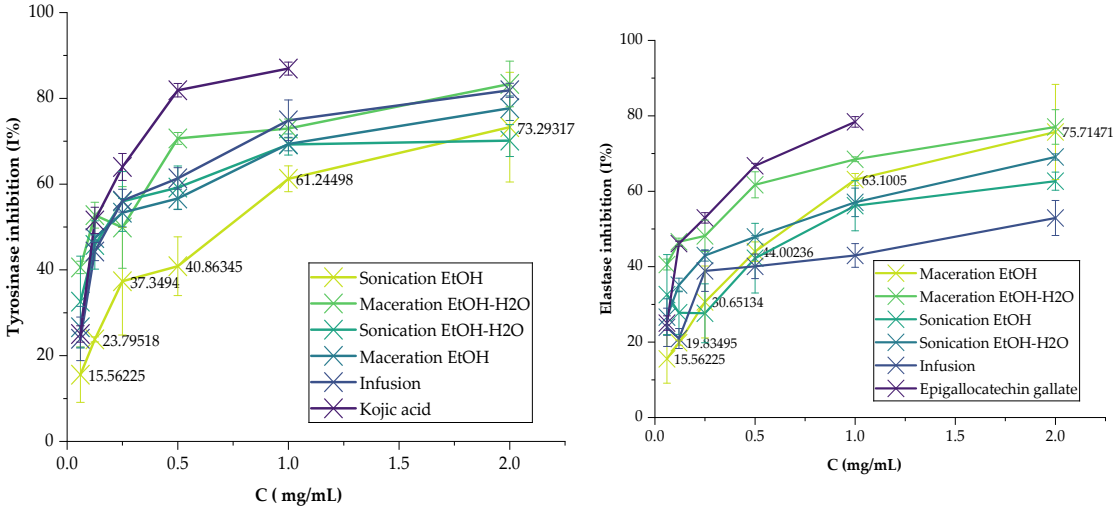

(**a**) (**b**)

Preprints.org (www.preprints.org) | NOT PEER-REVIEWED | Posted: 18 April 2025 doi:10.20944/preprints202504.1496.v1

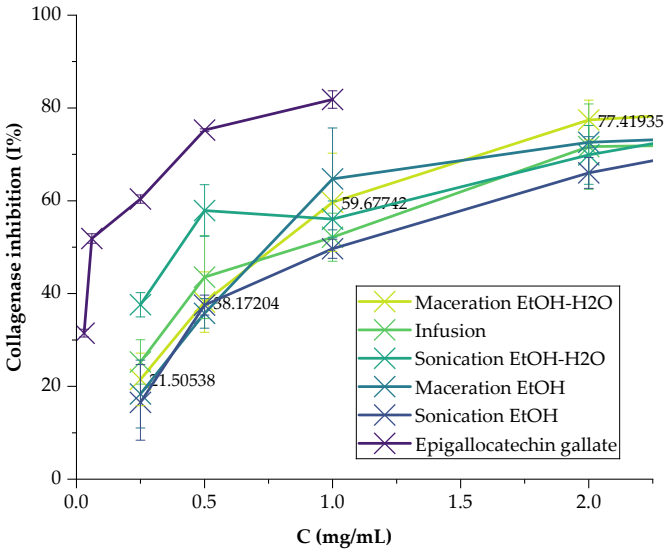

(c)

Figure 1. The inhibiting properties of *P. graveolens* flower extracts across tyrosinase (a), elastase (b) and collagenase (c) at various concentrations.

The aging process of skin often leads to a decline in its elasticity, primarily attributed to elastase activity. Elastase, an enzyme responsible for degrading elastin, a crucial protein governing the mechanical properties of connective tissues, becomes activated under stimuli such as UV rays and cytokines. This activation contributes to the degradation of elastic fibers, ultimately leading to the formation of wrinkles [31]. In parallel, collagenase, another key enzyme, plays a pivotal role in skin health. It is primarily responsible for breaking down collagen, a structural protein vital for skin firmness and elasticity [32]. Collagen and elastin, interconnected in maintaining skin structure and function, are susceptible to degradation when collagenase activity becomes dysregulated. Consequently, excessive collagen degradation can compromise skin firmness and tone, indirectly impacting elastin integrity.

Table 2. SPF values of *P. graveolens* extracts and IC50 values (mg/mL) against tyrosinase, elastase, collagenase and BSA denaturation.

Methods	Positive Controls	Sonication		Maceration		Infusion
		EtOH- H2O	EtOH	EtOH- H2O	EtOH	H2O
SPF	11.88 ± 2.088[1, a]	26.02 ± 0.020[b]	24.33 ± 0.15[b]	24.78 ± 0.127[b]	25.49 ± 0.016[b]	25.56 ± 0.059[b]
BSA (IC_{50} mg/mL)	0.175 ± 0.010[2, a]	0.20 ± 0.031[a]	0.61 ± 0.030[a]	0.44 ± 0.024[a]	0.38 ± 0.022[a]	1.64 ± 0.111[b]
Tyrosinase (IC_{50} mg/mL)	0.071 ± 0.013[3, a]	0.06 ± 0.079[a]	0.82 ± 0.306[b]	0.15 ± 0.103[a]	0.37 ± 0.017[a]	0.34 ± 0.070[a]
Elastase (IC_{50} mg/mL)	0.11 ± 0.003[4, a]	0.75 ± 0.011[b]	1.00 ± 0.309[b]	0.12 ± 0.100[b]	0.81 ± 0.155[b]	1.49 ± 0.243[b]
Collagenase (IC_{50} mg/mL)	0.08 ± 0.003[4, a]	0.52 ± 0.104[a c]	1.46 ± 0.137[b]	0.95 ± 0.139[a c d]	1.16 ± 0.275[d]	1.09 ± 0.187[c d]

Zinc Oxide[1], Diclofenac[2], Kojic acid [3], Epigallocatechin gallate[4]. Values are expressed as means ± standard error (n = 3). ANOVA followed by Tukey test. Values with different letters in the same row are significantly different ($p < 0.05$).

 doi:10.20944/preprints202504.1496.v1

All extracts of *P. graveolens* flower demonstrated a significant inhibition on elastase and collagenase enzymes (Figure 1), potentially due to the presence of inhibitory molecules, such as gallic acid, caffeic acid and quercetin. According to various studies by Wittenauer, et al, Loo et al and Deniz et al [33–35], these molecules can exhibit inhibitory activities against both elastase and collagenase. Notably, at 2 mg/mL both hydroethanolic extracts obtained via maceration (77.045 ± 4.578%) and sonication (69.094 ± 0.820%) exhibited dose-dependent inhibition of elastase enzyme; however, the maximum inhibition (78.395± 1.393%) was achieved by the standard anti-aging agent Epigallocatechin gallate at a concentration of 1 mg/mL (Figure 1 (b)). *P. graveolens* extracts displayed notable efficacy in inhibiting collagenase enzyme activity (Figure 1 (c)). The hydroethanolic maceration extract exhibited the highest inhibition, reducing 83.870± 4.267% of collagenase activity at 4 mg/mL and 21.505± 5.664% at 0.25 mg/mL. Similarly, hydroethanolic sonication inhibited 89.388±1.635 % of the enzyme at a concentration of 4 mg/mL and 37.600±2.620% at 0.25 mg/mL. This underlines their potential as competitive anti-aging ingredients compared with epigallocatechin gallate, which inhibited collagenase activity by up to 81.822 ± 1.876% at 1 mg/mL.

Elastase and collagenase inhibition activities were quantified similarly to IC_{50} values, as reported in Table 2. The lowest IC_{50} value for elastase inhibition was attributed to the hydroethanolic maceration extract (IC_{50} = 0.12 ± 0.100 mg/mL) and epigallocatechin gallate (IC_{50} = 0.03 ± 0.01 mg/mL), while the highest value was observed in the infusion extract (IC_{50} = 1.49 ± 0.243 mg/mL); however, no statistically significant difference was found between the values of the extract and Epigallocatechin gallate ($p < 0.05$). The hydroethanolic maceration extract, rich in polar free phenolic acids, showed, therefore, the most potent inhibitory activity. Gallic acid, with its three adjacent hydroxyl and carboxyl functional groups, appear to play a crucial role in these inhibitory effects [36,37]. For collagenase inhibition, hydroethanolic extracts by sonication and maceration displayed IC_{50} values of 0.52 ± 0.104 mg/mL and 0.95 ± 0.139 mg/mL, respectively. Furthermore, epigallocatechin gallate demonstrated a lowest IC_{50} value of 0.08 ± 0.0034 mg/mL. However, there was no significant difference between the positive control and extracts ($p > 0.05$). Other extracts, such as the water infusion, ethanolic maceration, and ethanolic sonication extracts, showed descending IC_{50} values of 1.09 ± 0.187 mg/mL, 1.16 ± 0.275 mg/mL, and 1.46 ± 0.137 mg/mL, respectively.

3.4. Photoprotective Activity

The Sun Protection Factor (SPF) or sometimes known simply as Protection Index (IP) is a measurement of the level of sun protection of a product and its ability to protect skin against UV radiations [38]. Ingredients with high SPF are indispensable in cosmetic and pharmaceutical preparation of anti-pigmentation and lightening products [39]. The crude extracts of *P. graveolens* have been evaluated for their efficacy in providing medium to high levels of protection. Among these, the extract obtained by hydroethanolic sonication, and the extract obtained by infusion exhibited the highest protective effects (26.02 ± 0.02 and 25.56 ± 0.059, respectively), while the extracts obtained by hydroethanolic maceration, hydroethanolic or ethanolic sonication provided close values (24.78 ± 0.127, 24.00 ± 4.39 and 24.33 ± 0.15, respectively) (Table 2). All extracts scored higher SPF than the positive control, zinc oxide (11.88 ± 2.088) ($p < 0.05$). A link between UVB exposure and collagen expression has been established in previous studies [40], indicating that prolonged exposure to UVB could lead to collagen degradation, and therefore contribute to skin aging. Therefore, polyphenols are widely used as a natural compound to protect the skin from damage caused by harmful UV radiation [41], acting as effective sunscreen agents. Their chromophore structure enables them to absorb UV radiation [42].

3.5. Interfacial and Surface Tension Characteristics

Hydroethanolic plant extracts can contain multiple surface-active molecules that contribute to the formation or stabilization of emulsions. Comprehensively, these molecules tend to adsorb at the air-water or oil-water interfaces due to their amphiphilic nature, reducing the surface or interfacial tension between immiscible phases and creating a physical barrier that prevents droplet aggregation or phase separation [43]. The extent at which surface-active compounds reduce the surface or

 doi:10.20944/preprints202504.1496.v1

interfacial tension and their speed or adsorption at the interface are both important to determine their surface-active potential. Usually, the higher and the faster is the interfacial tension reduction, the greater is the emulsifying ability and stability of emulsions [44]. The dynamic surface tension and interfacial tension of aqueous phases containing *P. graveolens* flower extracts were measured and presented in Figure 2. The surface tension and interfacial tension of air-water and soybean oil-water interfaces were 72 and 25 mN/m at time 0s and were reduced to about 70 and 19 mN/m at the end of the measurement. As shown in Figure 2, all extracts showed valuable activity in reducing interfacial tension and surface tension, indicating their potential to be used as a co-emulsifier or co-stabilizer of emulsions. Sonication extracts, for example, reduced the surface tension to approximately 48 mN/m at time 0s and 42 mN/m after 600 s. In addition, extracts obtained by maceration and ethanolic sonication reduced the interfacial tension to approximately 11 mN/m at time 0s and 8 mN/m after 600s. Infusion extract showed a lower reduction of interfacial tension and surface tension, possibly due to the milder conditions of the infusion process, which may not enhance the release of surface-active active compounds. The surface-active properties and composition of *P. graveolens* flower extracts have not been studied previously. The standard polysorbate 20, which is often used as emulsifier in dermo-cosmetic formulations, lowered the interfacial and surface tension to 6.93 mN/m and 43.22 mN/m, respectively. The initial reduction of tensions at time 0s was also significant, due to its small molecular size and therefore rapid diffusion to the interface. The results obtained in this study indicate, therefore, that *P. graveolens* flower extracts can be used as natural co-emulsifier in emulsion formulations.

3.6. Chemical Profiling: HPLC-PDA-MS/MS

In this study we visually selected the hydroethanolic extract as the most efficient for subsequent evaluation by chemical profiling. The LC-MS analysis unveiled a rich chemical profile. By meticulously scrutinizing molecular ions using extracted ion mass chromatograms and cross-referencing with available literature, several important compounds were identified. The extract was found to contain a total of 42 discernible compounds, consisting of five organic acids, 26 phenolic compounds, and 11 flavonoids. However, six compounds eluded identification despite exhaustive efforts. As presented in Table 3 and Figure 3, compound (4) displayed a prominent base peak with a protonated molecule [M - H]- observed at m/z 173, indicative of its molecular weight. This observation led to the identification of the compound as shikimic acid. The phenolic compound (5) exhibited a protonated molecule [M - H]- at m/z 493, accompanied by notable fragments at m/z 125 and 169. Further analysis revealed a loss of 324 amu from the pseudomolecular ion, suggesting the presence of two glucosides. Based on these findings, the compound was identified as Gallic acid diglucoside

 doi:10.20944/preprints202504.1496.v1

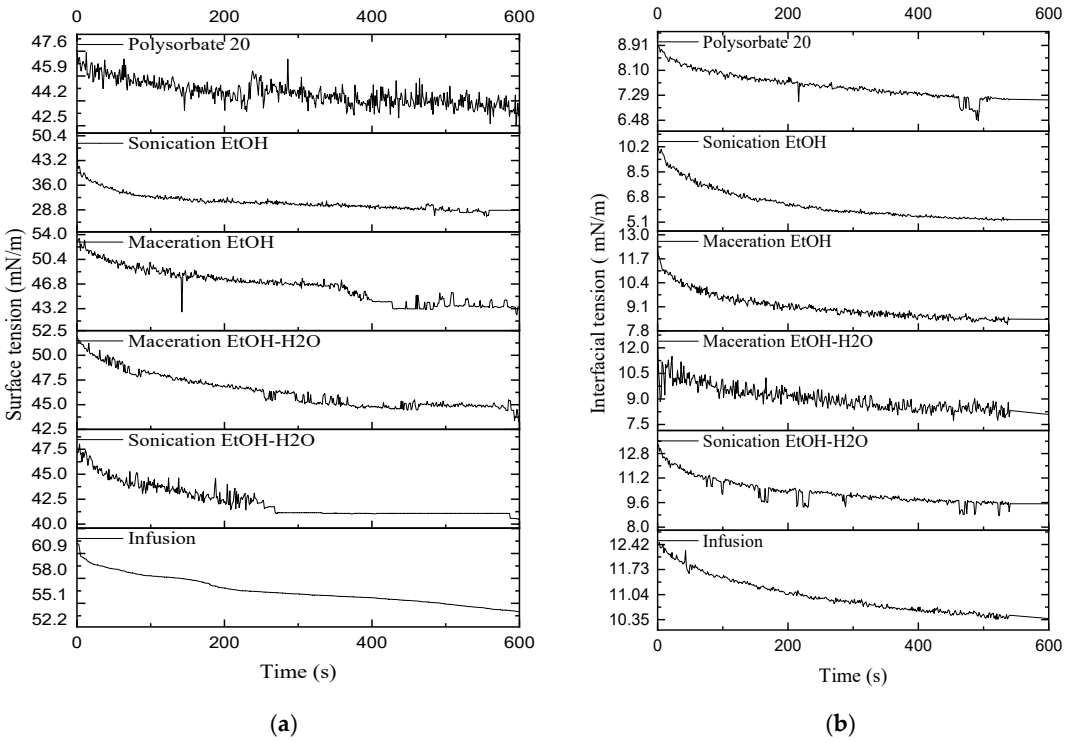

Figure 2. Over time, variations in interfacial tension (a) and surface tension (b) of *P. graveolens* flower extracts.

In the case of compound (7), a base peak [M - H]- was observed at m/z 371, along with fragments at m/z 167 and 197. This pattern of fragmentation led to the identification of the compound as Salvianolic Acid M. Compound (8) displayed a base peak [M - H]- at m/z 491, accompanied by fragments at m/z 167 and an aglycon ion at m/z 123. A loss of 324 amu from the pseudomolecular ion suggested the loss of two glucose molecules, leading to the identification of the compound as Vanillic acid diglucoside.

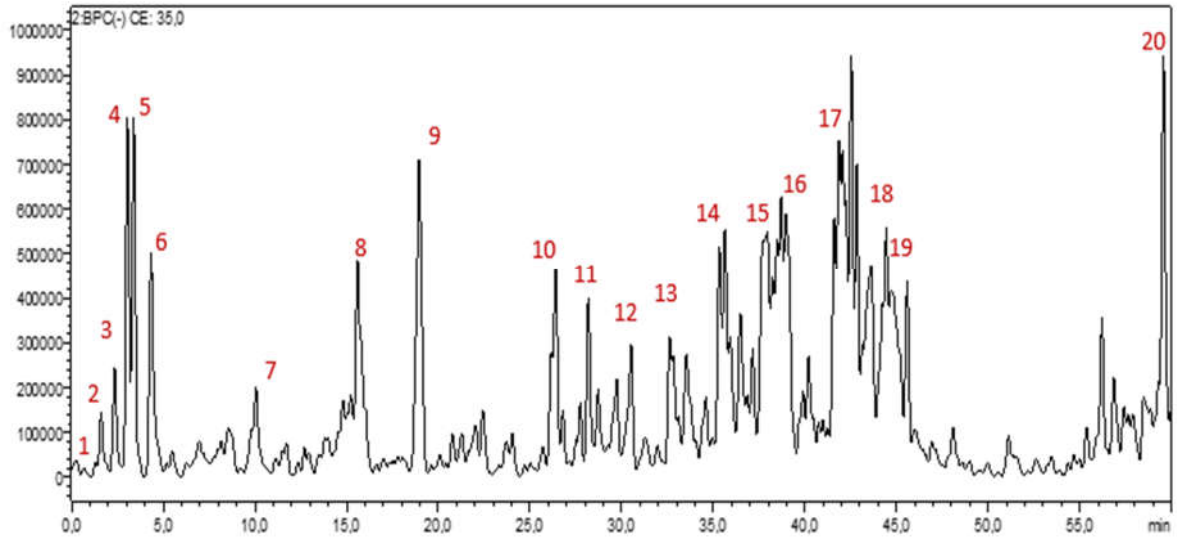

Figure 3. Identification of key compounds by LC-MS of hydroethanolic extract from *P. graveolens* flowers: 1: Tartaric acid, 2: Malic acid, 3: Shikimic acid, 4: Citric acid, 5: Gallic acid diglucoside, 6: Gallic acid, 7: Salvianolic Acid M, 8: Vanillic acid glucoside, 9: Eriodictiol glucoside pentoside, 10: Myrisetin glucoside rhamnoside, 11: Myricetin pentoside, 12: Kaempferol glucoside rhamnoside, 13: Quercetin pentoside, 14-17: non-identified,18: Kaempferol, 19: Isorhamnetin pentoside, 19: Isorhamnetin pentoside, 20: Cirsimaritin.

 doi:10.20944/preprints202504.1496.v1

Compound (9), with an [M-H]- ion at m/z 581 and significant fragments at m/z 287, indicated the presence of glucose and pentose. These observations, along with the obtained MS spectra, led to the identification of the compound as eriodictyol glucoside pentoside. Similarly, compound (10) exhibited a base peak [M - H]- at m/z 625, along with fragments at m/z 271 and m/z 317. The loss of 308 amu from the pseudomolecular ion suggested the loss of glucose and rhamnose, leading to the identification of the compound as myricetin glucoside rhamnoside. Compound (11) displayed a base peak [M - H]- at m/z 449, along with fragments at m/z 301 and m/z 317. The loss of m/z 132 from the pseudomolecular ion indicated the presence of a pentoside, identifying the compound as Myricetin pentoside. Compound (12) exhibited a base peak [M - H]- at m/z 593, with fragments at m/z 285 corresponding to the molecular weight of kaempferol. The loss of m/z 308 from the pseudomolecular ion suggested the loss of a glucose and a rhamnoside, identifying the compound as Kaempferol glucoside rhamnoside. Compound (18) displayed a base peak [M - H]- at m/z 285, indicating its molecular weight as that of kaempferol. Fragments at m/z 151 further supported this identification, confirming the compound as Kaempferol. Compound (19) exhibited a base peak [M - H]- at m/z 447, with fragments at m/z 315 indicating the loss of a pentoside. This led to the identification of the compound as Isorhamnetin pentoside. Finally, compound (20) displayed a base peak [M - H]- at m/z 313, corresponding to the molecular weight of cirsimaritin. Fragments at m/z 283 and m/z 295 further supported this identification, confirming the compound as cirsimaritin.

Table 3. Annotated compounds from *P. graveolens* hydroethanolic extract using LC-MS/MS.

Rt (min)	$[M-H]^-$	MS/MS	Proposed compounds
1.57	149	103	Tartaric acid
1.81	133	115	Malic acid
1.90	173	129	Shikimic acid
2.35	191	111	Citric acid
2.72	493	125, 169	Gallic acid diglucoside
2.83	331	125, 169	Gallic acid glucoside
4.27	169	125	Gallic acid
5.71	491	123, 167	Vanillic acid diglucoside
6.64	315	153	Protocatechuic acid glucoside
6.77	233	153	Dihydroxybenzoic acid sulfate
7.75	325	125, 169	Gallic acid shikimate
7.87	153	108	Dihydroxybenzoic acid
7.88	305	125, 179	Gallocatechin
9.48	483	169	Digallic acid glucoside
9.60	395	153, 315	Protocatechuic acid sulfoglucoside
10.54	371	167, 197	Quinylsyringic acid/ Salvianolic Acid M
11.24	341	135, 161, 179	Caffeic acid glucoside

 doi:10.20944/preprints202504.1496.v1

12.34	321	125, 169	Digallic acid
13.08	295	125, 169	Gallic acid triacetate
15.22	329	167	Vanillic acid glucoside
18.78	581	287, 447	Eriodictyol glucoside pentoside
20.59	633	169, 301, 463	Unknown
21.04	467	153, 169	Dihydroxybenzoic acid galloyl glucoside
22.19	197	125, 169	Syringic Acid
25.97	473	169, 321	Trigallic Acid
26.12	479	271, 317	Myricetin glucoside
26.41	625	271, 317	Myricetin glucoside rhamnoside
27.85	595	271, 301	Quercetin glucoside pentoside
28.95	449	301, 317	Myricetin pentoside
29.49	463	301, 317	Myricetin rhamnoside
29.49	609	271, 301	Quercetin rutinoside
30.35	463	301	Quercetin glucoside
30.55	593	285	Kaempferol glucoside rhamnoside
31.17	579	285	Kaempferol glucoside pentoside
32.07	565	271, 301	Quercetin dipentoside
32.93	433	271, 301	Quercetin pentoside
34.53	447	255, 285	Kaempferol glucoside
34.57	623	301, 315	Isorhamnetin glucoside rhamnoside
34.74	287	259	Eriodictyol
35.32	545	125, 169, 241	Unknown
37.85	621	125, 169, 241	Unknown
39.86	697	169, 317, 469, 617	Unknown
41.01	773	169, 241, 317, 493, 617	Unknown
44.17	285	151	Kaempferol
45.61	447	315	Isorhamnetin pentoside
50.70	315	315	Isorhamnetin

 doi:10.20944/preprints202504.1496.v1

56.19	313	283, 295	Cirsimaritin

RT: Retention time.

Boukhris et al. [45] analyzed the chemical composition of methanolic and aqueous extracts from *Pelargonium* flowers in positive mode. Five compounds were identified in the aqueous extract and four in the methanolic extract, primarily consisting of myricetin, quercetin, kaempferol, and isorhamnetin aglycone. The phenolic compounds present in the extract, including gallic acid derivatives like gallic acid diglucoside, possessed potent antioxidant properties [46]. Phenolic acids such as protocatechuic acid, syringic acid, caffeic acid and vanillic acid, along with their derivatives, exhibited anti-inflammatory [47,48], antimicrobial and anticancer activities [49,50]. Furthermore, Compounds like quercetin, kaempferol, myricetin, and apigenin glycosides are renowned for their antioxidant properties [51–54]. Organic acids identified in the extract, including tartaric acid, malic acid, shikimic acid, and citric acid, also contributed potentially to its physiological properties and functionality [55–57]. These acids play crucial roles in various processes and are valued in pharmaceutical and cosmetic formulations [58,59]. The presence of these bioactive compounds underscores the potential therapeutic applications of the hydroethanolic extract from *P. graveolens* flower.

3.7. Binding Site Prediction

The Bovine Serum Albumin (BSA) Denaturation Inhibition Assay is a widely used in vitro method for evaluating the anti-inflammatory potential of compounds. This assay is based on the principle that protein denaturation leads to inflammation, mirroring the protein aggregation observed in inflammatory conditions [60]. In this in silico study, Trigallic Acid, Salvianolic Acid M, and Gallic acid triacetate were the most active molecules in binding to this protein with a glide gscore of -8.321, -7.665, and -7.001Kcal/mol (Table 1). In the other hand, Shikimic acid, Dihydroxybenzoic acid, and Syringic acid exhibited the highest tyrosinase inhibitory activity, with glide scores of -8.116, -7.966, and -7.905 kcal/mol, respectively (Table 4).

Collagenase and elastase are two critical proteolytic enzymes responsible for the degradation of collagen and elastin, essential structural proteins in the skin. Their overactivity accelerates skin aging, leading to wrinkles and loss of firmness [61]. *P. graveolens* extracts demonstrated significant in vitro inhibitory activity against elastase collagenase and tyrosinase enzymes. To further elucidate the binding mode and affinity of the major components of its extract toward these enzymes, computational approaches were employed. Molecular docking analysis revealed that Shikimic acid, Protocatechuic acid glucoside, and Dihydroxybenzoic acid as the most potent collagenase inhibitors, with glide scores of -9.100, -8.622, and -8.532 kcal/mol, respectively. For elastase inhibition, Dihydroxybenzoic acid, Myricetin pentoside, and Quercetin rutinoside demonstrated the highest activity, with glide scores of -5.381, -5.264, and -5.195 kcal/mol, respectively (Table 4).

Table 4. In silico binding site prediction results in different receptors.

Compounds	**Glide gscore (Kcal/mol)**			
	Tyrosinase (PDB :2Y9X)	Collagenase (PDB : 2TCL)	Elastase (PDB: 7EST)	BSA (PDB: 6QS9)
Caffeic acid glucoside	-6.22	-5.817	-4.292	-5.667
Cirsimaritin	-	-5.281	-4.2	-5.885
Citric acid	-6.071	-7.165	-4.832	-5.014
Digallic acid	-7.277	-7.704	-4.121	-6.361
Dihydroxybenzoic acid	-7.966	-8.532	-5.381	-6.235
Eriodictyol	-6.814	-7.657	-4.705	-6.041

 doi:10.20944/preprints202504.1496.v1

Gallic acid	-7.518	-7.828	-4.924	-6.137
Gallic acid glucoside	-7.219	-5.804	-4.092	-5.949
Gallic acid triacetate	-6.181	-7.367	-4.538	-7.001
Gallocatechin	-6.822	-8.548	-3.562	-6.703
Isorhamnetin	-5.979	-6.308	-4.61	-6.111
Isorhamnetin glucoside	-5.443	-5.924	-4.094	
Kaempferol	-5.862	-5.79	-5.191	-5.961
Kaempferol glucoside	-5.358	-6.028	-4.73	-6.224
Malic acid	-6.109	-7.032	-4.567	-4.036
Myricetin glucoside	-4.35	-6.365	-4.339	-6.844
Myricetin pentoside	-6.985	-7.242	-5.264	-5.91
Myricetin rhamnoside	-6.351	-7.265	-5.144	-6.497
Protocatechuic acid glucoside	-7.372	-8.622	-4.799	-6.951
Quercetin glucoside	-4.465	-6.918	-4.764	-5.873
Quercetin rutinoside	-5.329	-8.184	-5.195	-
Salvianolic Acid M	-5.324	-7.943	-4.808	-7.665
Shikimic acid	-8.116	-9.1	-4.887	-6.097
Syringic Acid	-7.905	-7.828	-4.267	-6.368
Tartaric acid	-5.709	-7.519	-4.459	-4.283
Trigallic Acid	-7.004	-9.146	-5.046	-8.321
Vanillic acid	-7.661	-7.96	-4.217	-6.725
Vanillic acid glucoside	-6.983	-8.22	-4.516	-5.504

In the active site of Bovine Serum Albumin, Trigallic Acid established six hydrogen bonds with residues GLU 152, TYR 149, ARG 256, SER 286, ILE 289, and ARG 217 and one Pi-Pi cation with residue TYR 149 and Pi-stacking bonds with residue ARG 198, and one salt bridge with residue ARG 217. (Figures 4 (a) and 5 (a)).

Moreover, Shikimic acid established one hydrogen bond with residue CU400 (Figures 4 (c) and 5 (c)). Similarly, the molecule established four hydrogen bonds with residues ALA 82, LEU 81, and PRO 138, and one salt bridge with residue ZN 170 (Figures 4 (c) and 5 (c)).

In the active site of elastase, Dihydroxybenzoic acid formed three hydrogen bonds with residuesTHR 20 and TYR 159 and one salt bridge with residue ARG 188 (Figures 4 (d) and 5(d)).

Preprints.org (www.preprints.org) | NOT PEER-REVIEWED | Posted: 18 April 2025 doi:10.20944/preprints202504.1496.v1

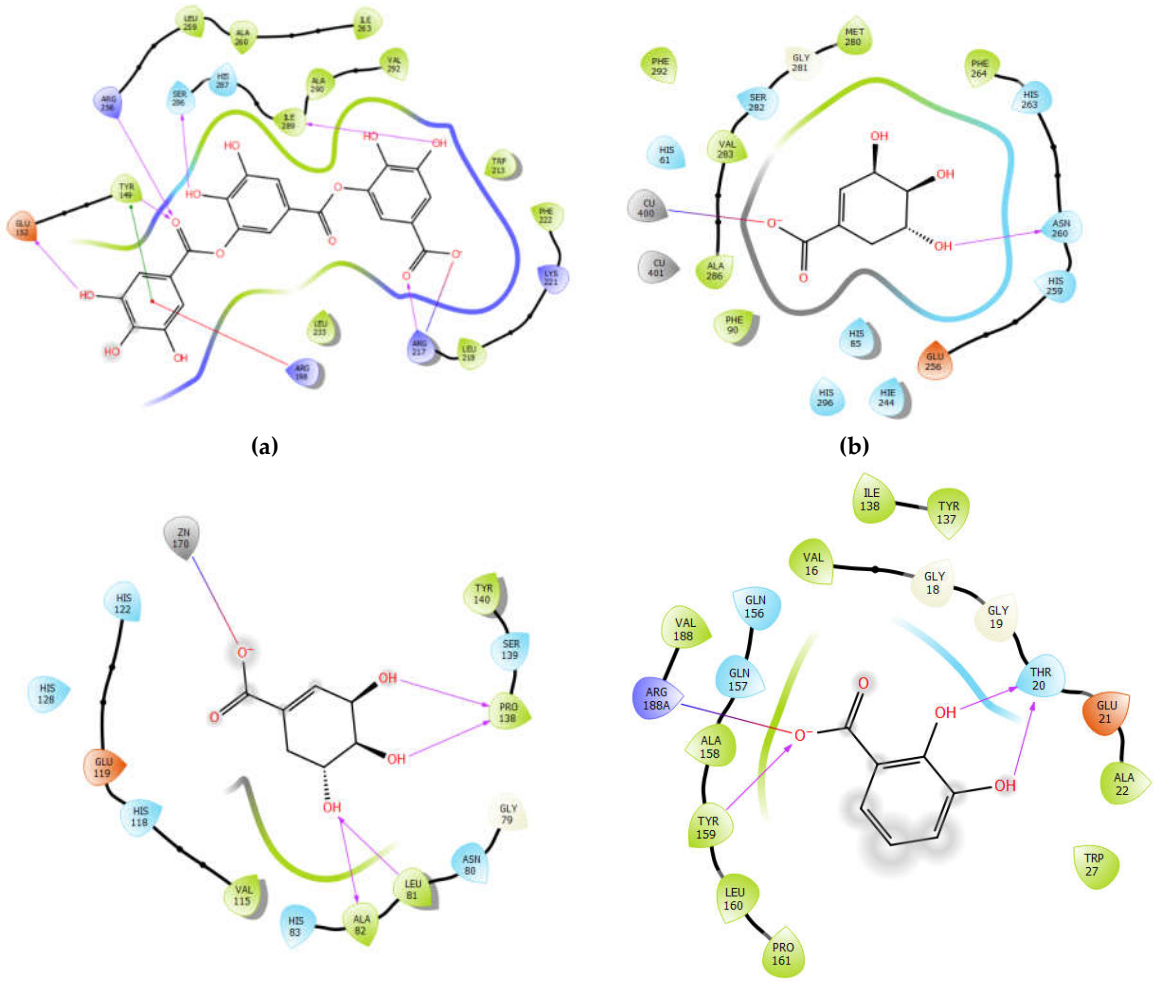

Figure 4. The 2D viewer of ligands interactions with the active site. (a): Trigallic Acid interactions with active site of bovine serum albumin. (b and c): Shikimic acid interactions with tyrosinase and collagenase active sites. (d): Dihydroxybenzoic acid interactions with elastase active sites.

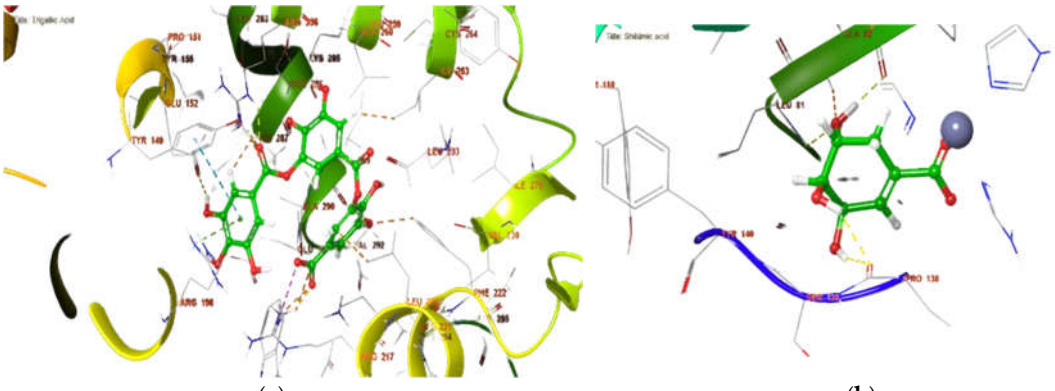

 doi:10.20944/preprints202504.1496.v1

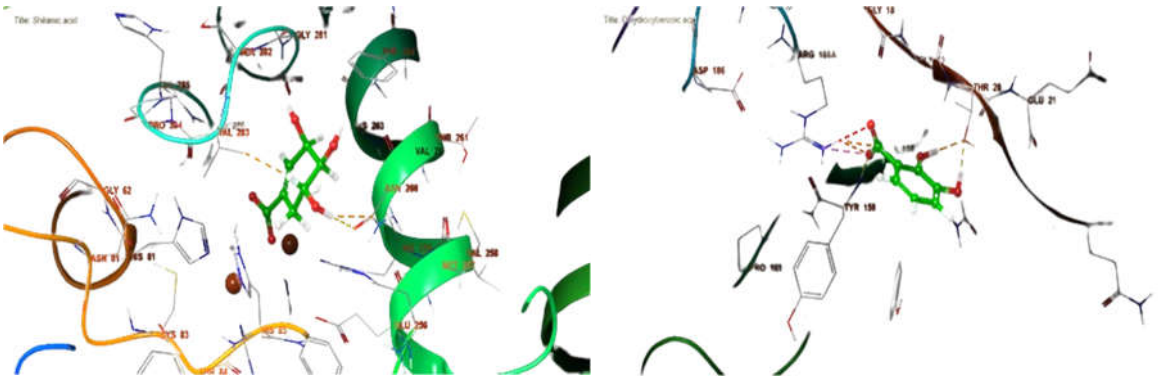

(**c**) (**d**)

Figure 5. The 3D viewer of ligands interactions with the active site. (a): Trigallic Acid interactions with active site of bovine serum albumin. (b and c): Shikimic acid interactions with tyrosinase and collagenase active sites. (d): Dihydroxybenzoic acid interactions with elastase active sites.

3.8. Application: Aqueous Serum Formulas

3.8.1. Stability

Following the production of the aqueous face serums (F1, F2, and F3), their stability was assessed through various tests over a 3-month period. Accelerated stability assays were conducted to gauge the products' performance under extreme conditions. Upon centrifugation, both face serums F1 and F2 maintained their homogeneity without any phase separation, indicating stability and consistency throughout the testing period. However, F3 exhibited phase separation, potentially due to the need for a co-stabilizer. the surface activity of *P. graveolens* extract may have been insufficient to sustain physical stability in this formula. Furthermore, none of the serums showed phase separation after the thermal stability test, although minor weight variations were noted. Despite this, all organoleptic properties, appearance, and homogeneity remained unaffected for F1 and F2, confirming their stability against mechanical and temperature stress. This was not observed for F3. However, the interfacial and surface tension effects of the selected *P. graveolens* extract could help stabilize the formulas and prevent coalescence.

Regarding the chemical stability of the formulated cosmetic serums, encompassing parameters such as water activity, conductivity, peroxide value, and pH, their fluctuations over a span of 90 days are depicted in Figure 6. This graphical representation delineates the alterations in water activity (A), conductivity (B), pH (C), and peroxide values (D) across the three formulations during the specified timeframe. As depicted in Figure 6, it is evident that the fluctuations in water activity and conductivity of the samples remained minimal over the 90-day period. Additionally, there were only slight alterations observed in the pH values across the various assays. However, it is worth noting that the pH of healthy skin typically falls within the range of 5 to 6.0 indicating compatibility with skin.

Regarding conductivity measurements of the face serums formulas, F1 exhibited a range from 747.60 ± 1.53 µS/cm at the time of preparation to 640.3 ± 1.53 µS/cm after 90 days. F2 started at 700.50 ± 601.50 µS/cm and decreased to 601.56 ± 1.25 µS/cm after 90 days. Similarly, F3 initially registered a conductivity of 1044.00 ± 1.00 µS/cm, showing a slight decrease to 1009.00 ± 1.15 µS/cm after 90 days. These values showed minimal variation over time ($p < 0.05$). Previously, Latreille et al [62] have demonstrated a correlation between conductivity and stability, enabling accurate assessment of shelf life.

Figure 6 (d) illustrates peroxide value of three cosmetic serums formulas from day 1 to day 90. The analysis revealed consistently low peroxide values across all formulations. After 90 days, the highest value ($p < 0.05$) was observed in F2 (0.82 ± 0.01 mEq/kg), followed by F3 (0.62 ± 0.01 mEq/kg) and F1 (0.50 ± 0.01 mEq/kg). However, there were statistically no significant variations observed from preparation through 15, 30, 60, and 90 days ($p > 0.05$). This suggests that the minimal oxidation values

 doi:10.20944/preprints202504.1496.v1

may be attributed to the aqueous composition devoid of significant fatty acids or to the antioxidant effect of the active extract from *P. graveolens* flower.

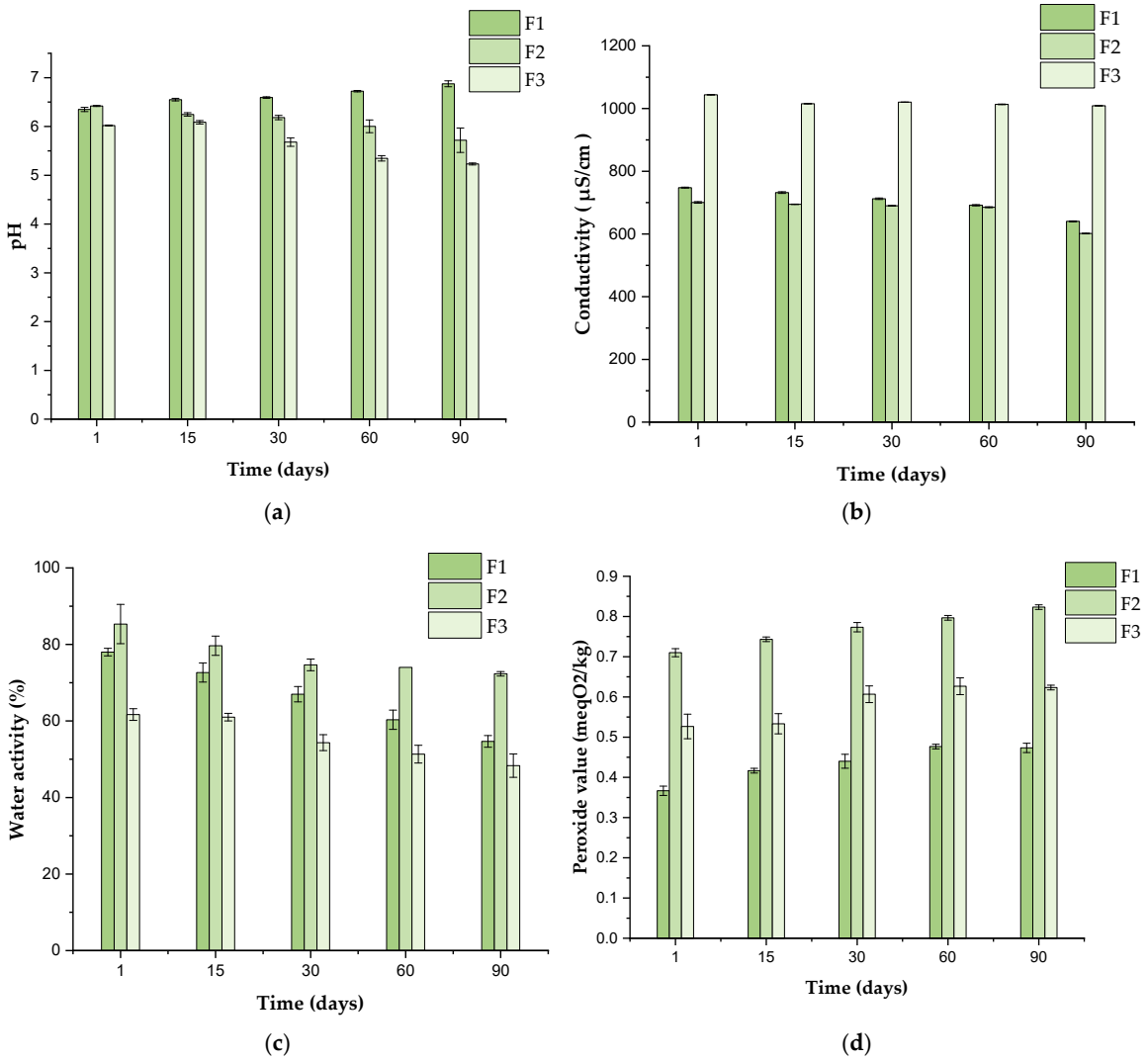

Figure 6. Chemical stability of formulated cosmetic serums over three months: (a) pH values, (b) conductivity, (c) water activity, and (d) peroxide values.

4. Conclusions

The study investigates *P. graveolens* flower extracts for potential applications in dermo-cosmetics and pharmaceuticals. Phytochemical analysis by HPLC-PDA-MS/MS revealed key compounds including shikimic acid, gallic acid diglucoside, salvianolic acid M, and others, known for their anti-inflammatory, and antimicrobial properties. *P. graveolens* flower extracts are valuable for skincare formulations targeting skin pigmentation by inhibiting tyrosinase enzyme and skin disorders associated with skin aging by inhibiting elastase and collagenase enzymes. Furthermore, antifungal assays showed efficacy against various dermatophytes and pathogenic yeasts, notably isolated from patients affected by tinea capitis and onychomycosis. In terms of a pharmaceutical application, F1 and F2 aqueous serums demonstrated better stability. Yet, further research is needed to isolate the active compounds from *P. graveolens* sonication flower extract and elucidate their inhibitory pathways.

Funding: This research received no external funding

Institutional Review Board Statement: Ethical review and approval were waived due to the retrospective character of the study and the fact that no personal information was required for this study.

 doi:10.20944/preprints202504.1496.v1

Informed Consent Statement: Patient consent was waived due to the retrospective character of the study and the fact that no personal information was required for this study.

Data Availability Statement: The project includes the following underlying datasets, Raw_Data_P.graveolens/BSA_Denaturation.xlsx, Raw_Data_P.graveolens/Enzyme Inhibition.xlsx, Raw_Data_P.graveolens/Photoprotecteur_SPF.xlsx, Raw_Data_P.graveolens/Spectrus.pdf, Available at DOI: 10.6084/m9.figshare.28714856 [63]. The data are provided under the Creative Commons Zero (CC0 1.0) Public Domain Dedication, with no rights reserved.

Acknowledgments: The authors would like to express their gratitude to the University Hospital Center Hassan II and the entire Parasitology and Mycology Department of the central laboratory of medical analysis team for their valuable contribution to this research project. The authors would also like to thank Mr. Rachid ELMENAOUAR, a professor of English at the Higher Institute of Nursing Professions and Health Techniques, Rabat, Ministry of Health and Social Protection, Morocco, for his meticulous review and suggestions on the manuscript. And Pr. Hamid Khamar from the Botanical Department of the Scientific Institute of Rabat, Morocco, for the authentication of the plant.

Conflicts of Interest: The authors declare no conflicts of interest.

References

1. Kumar MA. The skin. Techniques in Small Animal Wound Management. 2024:1.
2. Elbuluk N, Grimes P, Chien A, Hamzavi I, Alexis A, Taylor S, et al. The pathogenesis and management of acne-induced post-inflammatory hyperpigmentation. American journal of clinical dermatology. 2021;22(6):829-36.
3. Karkoszka M, Rok J, Wrześniok D. Melanin Biopolymers in Pharmacology and Medicine—Skin Pigmentation Disorders, Implications for Drug Action, Adverse Effects and Therapy. Pharmaceuticals. 2024;17(4):521.
4. Zolghadri S, Bahrami A, Hassan Khan MT, Munoz-Munoz J, Garcia-Molina F, Garcia-Canovas F, et al. A comprehensive review on tyrosinase inhibitors. Journal of enzyme inhibition and medicinal chemistry. 2019;34(1):279-309.
5. Habachi E, Rebey IB, Dakhlaoui S, Hammami M, Sawsen S, Msaada K, et al. Arbutus unedo: Innovative Source of Antioxidant, Anti-Inflammatory and Anti-Tyrosinase Phenolics for Novel Cosmeceuticals. Cosmetics. 2022;9(6):143.
6. Fonseca S, Amaral MN, Reis CP, Custódio L. Marine Natural Products as Innovative Cosmetic Ingredients. Marine Drugs. 2023;21(3):170.
7. Fecker R, Magyari-Pavel IZ, Cocan I, Alexa E, Popescu IM, Lombrea A, et al. Oxidative Stability and Protective Effect of the Mixture between Helianthus annuus L. and Oenothera biennis L. Oils on 3D Tissue Models of Skin Irritation and Phototoxicity. Plants. 2022;11(21):2977.
8. Arraiza MP, Calderón-Guerrero C, Guillén SC, Sarmiento MA. Industrial Uses of MAPs: Cosmetic Industry. Medicinal and Aromatic Plants: The Basics of Industrial Application. 2017;1:30-44.
9. Savary G, Grisel M, Picard C. Cosmetics and personal care products. Natural polymers: industry techniques and applications. 2016:219-61.
10. Patil M, Joshi M, Kadam J, Zambare V, Sinha S, Pawar R, et al. Application as cosmetic bioactives of phytochemicals extracted from the post distillation biomass of geranium. Songklanakarin Journal of Science & Technology. 2022;44(5).
11. Asgarpanah J, Ramezanloo F. An overview on phytopharmacology of Pelargonium graveolens L. 2015.
12. El-Otmani N, Zeouk I, Hammani O, Zahidi A. Analysis and Quality Control of Bio-actives and Herbal Cosmetics: The Case of Traditional Cooperatives from Fes-Meknes Region. Tropical Journal of Natural Product Research (TJNPR). 2024;8(5):7181-95.
13. Lekouaghet A, Boutefnouchet A, Bensuici C, Gali L, Ghenaiet K, Tichati L. In vitro evaluation of antioxidant and anti-inflammatory activities of the hydroalcoholic extract and its fractions from Leuzea conifera L. roots. South African Journal of Botany. 2020;132:103-7.

 doi:10.20944/preprints202504.1496.v1

14. Al-Mijalli SH, Mrabti HN, Assaggaf H, Attar AA, Hamed M, Baaboua AE, et al. Chemical profiling and biological activities of pelargonium graveolens essential oils at three different phenological stages. Plants. 2022;11(17):2226.
15. Khatib S, Mahdi I, Drissi B, Fahsi N, Bouissane L, Sobeh M. Tetraclinis articulata (Vahl) Mast.: Volatile constituents, antioxidant, antidiabetic and wound healing activities of its essential oil. Heliyon. 2024;10(3).
16. Kim Y-J, Uyama H, Kobayashi S. Inhibition effects of (+)-catechin–aldehyde polycondensates on proteinases causing proteolytic degradation of extracellular matrix. Biochemical and biophysical research communications. 2004;320(1):256-61.
17. Mansur JdS, Breder MNR, Mansur MCdA, Azulay RD. Determinação do fator de proteção solar por espectrofotometria. An Bras Dermatol. 1986:121-4.
18. Chebaibi M, Bourhia M, Slighoua M, Mssillou I, Aboul-Soud MA, Khalid A, et al. Salsoline Derivatives, Genistein, Semisynthetic Derivative of Kojic Acid, and Naringenin as inhibitors of A42R Profilin-like Protein of Monkeypox Virus: In Silico studies. Frontiers in Chemistry. 2024;12:1445606.
19. Tourabi M, Nouioura G, Touijer H, Baghouz A, El Ghouizi A, Chebaibi M, et al. Antioxidant, Antimicrobial, and Insecticidal Properties of Chemically Characterized Essential Oils Extracted from Mentha longifolia: In Vitro and In Silico Analysis. Plants. 2023;12(21):3783.
20. Meryem MJ, Agour A, Allali A, Chebaibi M, Bouia A. Chemical composition, free radicals, pathogenic microbes, α-amylase and α-glucosidase suppressant proprieties of essential oil derived from Moroccan Mentha pulegium: in silico and in vitro approaches. Journal of Biology and Biomedical Research. 2024;1(1):46-61.
21. Taibi M, Rezouki S, Moubchir T, El Abdali Y, Mssillou I, El Barnossi A, et al. Satureja calamintha essential oil: Chemical composition and assessing insecticidal efficacy through activity against acetylcholinesterase, chitin, juvenile hormone, and molting hormone. Journal of Biology and Biomedical Research (ISSN: 3009-5522). 2024;1(2):79-91.
22. Beniaich G, Hafsa O, Maliki I, Bin Jardan YA, El Moussaoui A, Chebaibi M, et al. GC-MS characterization, in vitro antioxidant, antimicrobial, and in silico nadph oxidase inhibition studies of anvillea radiata essential oils. Horticulturae. 2022;8(10):886.
23. Chebaibi M, Mssillou I, Allali A, Bourhia M, Bousta D, Gonçalves RFB, et al. Antiviral Activities of Compounds Derived from Medicinal Plants against SARS-CoV-2 Based on Molecular Docking of Proteases. Journal of Biology and Biomedical Research. 2024;1(1):10-30.
24. Ferreira SM, Santos L. A potential valorization strategy of wine industry by-products and their application in cosmetics—Case study: Grape pomace and grapeseed. Molecules. 2022;27(3):969.
25. Bezerra JJL, de Oliveira AFM. Exploring the therapeutic potential of Brazilian medicinal plants for anti-arthritic and anti-osteoarthritic applications: A comprehensive review. Biocatalysis and Agricultural Biotechnology. 2024:103064.
26. Afonso AF, Pereira OR, Cardoso SM. Health-promoting effects of Thymus phenolic-rich extracts: Antioxidant, anti-inflammatory and antitumoral properties. Antioxidants. 2020;9(9):814.
27. Martins CAF, Campos ML, Irioda AC, Stremel DP, Trindade ACLB, Pontarolo R. Anti-inflammatory effect of Malva sylvestris, Sida cordifolia, and Pelargonium graveolens is related to inhibition of prostanoid production. Molecules. 2017;22(11):1883.
28. El Aanachi S, Gali L, Nacer SN, Bensouici C, Dari K, Aassila H. Phenolic contents and in vitro investigation of the antioxidant, enzyme inhibitory, photoprotective, and antimicrobial effects of the organic extracts of Pelargonium graveolens growing in Morocco. Biocatalysis and Agricultural Biotechnology. 2020;29:101819.
29. Mukherjee PK, Biswas R, Sharma A, Banerjee S, Biswas S, Katiyar C. Validation of medicinal herbs for anti-tyrosinase potential. Journal of herbal medicine. 2018;14:1-16.
30. Zengin G, Locatelli M, Carradori S, Mocan AM, Aktumsek A. Total phenolics, flavonoids, condensed tannins content of eight Centaurea species and their broad inhibitory activities against cholinesterase, tyrosinase, α-amylase and α-glucosidase. Notulae Botanicae Horti Agrobotanici Cluj-Napoca. 2016;44(1):195-200.
31. Garg C. Molecular mechanisms of skin photoaging and plant inhibitors. International Journal of Green Pharmacy (IJGP). 2017;11(02).

 doi:10.20944/preprints202504.1496.v1

32. Nascimento NS, Torres-Obreque KM, Oliveira CA, Rabelo J, Baby AR, Long PF, et al. Enzymes for dermatological use. Experimental Dermatology. 2024;33(1):e15008.
33. Wittenauer J, Mäckle S, Sußmann D, Schweiggert-Weisz U, Carle R. Inhibitory effects of polyphenols from grape pomace extract on collagenase and elastase activity. Fitoterapia. 2015;101:179-87.
34. Loo YC, Hu H-C, Yu S-Y, Tsai Y-H, Korinek M, Wu Y-C, et al. Development on potential skin anti-aging agents of Cosmos caudatus Kunth via inhibition of collagenase, MMP-1 and MMP-3 activities. Phytomedicine. 2023;110:154643.
35. Deniz FSS, Salmas RE, Emerce E, Cankaya IIT, Yusufoglu HS, Orhan IE. Evaluation of collagenase, elastase and tyrosinase inhibitory activities of Cotinus coggygria Scop. through in vitro and in silico approaches. South African Journal of Botany. 2020;132:277-88.
36. Bai J, Zhang Y, Tang C, Hou Y, Ai X, Chen X, et al. Gallic acid: Pharmacological activities and molecular mechanisms involved in inflammation-related diseases. Biomedicine & pharmacotherapy. 2021;133:110985.
37. Ocampo-Gallego JS, Pedroza-Escobar D, Caicedo-Ortega AR, Berumen-Murra MT, Novelo-Aguirre AL, de Sotelo-León RD, et al. Human neutrophil elastase inhibitors: Classification, biological-synthetic sources and their relevance in related diseases. Fundamental & Clinical Pharmacology. 2023.
38. He H, Li A, Li S, Tang J, Li L, Xiong L. Natural components in sunscreens: Topical formulations with sun protection factor (SPF). Biomedicine & pharmacotherapy= Biomedecine & pharmacotherapie. 2020;134:111161-.
39. Gonçalves S, Gaivão I. Natural Ingredients in Skincare: A Scoping Review of Efficacy and Benefits.
40. Threskeia A, Sandhika W, Rahayu RP. Effect of turmeric (Curcuma longa) extract administration on tumor necrosis factor-alpha and type 1 collagen expression in UVB-light radiated BALB/c mice. J Appl Pharm Sci. 2023;13(5):121-5.
41. Bharadvaja N, Gautam S, Singh H. Natural polyphenols: a promising bioactive compounds for skin care and cosmetics. Molecular Biology Reports. 2023;50(2):1817-28.
42. Rajasekar M, Mary J, Sivakumar M, Selvam M. Recent developments in sunscreens based on chromophore compounds and nanoparticles. RSC advances. 2024;14(4):2529-63.
43. Taarji N, Bouhoute M, Chafai Y, Hafidi A, Kobayashi I, Neves MA, et al. Emulsifying performance of crude surface-active extracts from liquorice root (Glycyrrhiza glabra). ACS Food Science & Technology. 2021;1(8):1472-80.
44. Amine C, Dreher J, Helgason T, Tadros T. Investigation of emulsifying properties and emulsion stability of plant and milk proteins using interfacial tension and interfacial elasticity. Food Hydrocolloids. 2014;39:180-6.
45. Boukhris M, Simmonds MS, Sayadi S, Bouaziz M. Chemical composition and biological activities of polar extracts and essential oil of rose-scented geranium, Pelargonium graveolens. Phytotherapy research. 2013;27(8):1206-13.
46. Abdelouhab K, Guemmaz T, Karamać M, Kati DE, Amarowicz R, Arrar L. Phenolic composition and correlation with antioxidant properties of various organic fractions from Hertia cheirifolia extracts. Journal of Pharmaceutical and Biomedical Analysis. 2023;235:115673.
47. Rezig K, Benkaci-Ali F, Foucaunier ML, Laurent S, Umar HI, Alex OD, et al. HPLC/ESI-MS Characterization of Phenolic Compounds from Cnicus benedictus L. Roots: A Study of Antioxidant, Antibacterial, Anti-Inflammatory, and Anti-Alzheimer's Activity. Chemistry & Biodiversity. 2024;21(1):e202300724.
48. Chen Q, Yang Z-R, Du S, Chen S, Zhang L, Zhu J. Polyphenol-sodium alginate supramolecular injectable hydrogel with antibacterial and anti-inflammatory capabilities for infected wound healing. International Journal of Biological Macromolecules. 2024;257:128636.
49. Malathi V, Kanika S, Jinu J, Venkateswarlu R, Deepa M, Rohini A. 43 Phenolic Phytochemicals from Sorghum, Millets, and Pseudocereals and Their Role in Human Health. Nutriomics of Millet Crops: CRC Press; 2024. p. 43-80.
50. Nasrabadi NS, Vedad A, Asadi K, Poorbagher MRM, Tabrizi NA, Dorooki K, et al. Nanoliposome-loaded phenolics from Salvia leriifolia Benth and its anticancer effects against induced colorectal cancer in mice. Biotechnology and Applied Biochemistry. 2024.

 doi:10.20944/preprints202504.1496.v1

51. Kalaba M, Tešić Ž, Blagojević S. Flavonoids in Pollen. Pollen Chemistry & Biotechnology: Springer; 2024. p. 127-45.
52. Elshamy S, Handoussa H, El-Shazly M, Mohammed ED, Kuhnert N. Metabolomic profiling and quantification of polyphenols from leaves of seven Acacia species by UHPLC-QTOF-ESI-MS. Fitoterapia. 2024;172:105741.
53. Chomphen L, Yamanont P, Morales NP. Flavonoid Metabolites in Serum and Urine after the Ingestion of Selected Tropical Fruits. Nutrients. 2024;16(1):161.
54. Sunil C, Gowda NN, Nayak N, Rawson A. Unveiling the effect of processing on bioactive compounds in millets: Implications for health benefits and risks. Process Biochemistry. 2024.
55. Przybylska D, Kucharska AZ, Piórecki N, Sozański T. The Health-Promoting Quality Attributes, Polyphenols, Iridoids and Antioxidant Activity during the Development and Ripening of Cornelian Cherry (Cornus mas L.). Antioxidants. 2024;13(2):229.
56. Su T, Zhao J, Zhu Y, Oyom W, Li S, Xie P, et al. Comparison of nutrient composition, phytochemicals and antioxidant activities of two large fruit cultivars of sea buckthorn in Xinjiang of China. Scientia Horticulturae. 2024;324:112602.
57. Gao Q, Li X, Chang Y, Ma R, Cao X, Wang S. Dynamics of Physicochemical Characteristics, Bioactive Substances and Microbial Communities in Lycium Ruthenicum Murr. Compound Jiaosu During Spontaneous Fermentation. Compound Jiaosu During Spontaneous Fermentation.
58. Kebede I, Gebremeskel H, Ahmed A. Bee products and their processing: a review. Pharm Pharmacol Int J. 2024;12(1):5-12.
59. Romero-Orejon FL, Huaman J, Lozada P, Ramos-Escudero F, Muñoz AM. Development and Functionality of Sinami (Oenocarpus mapora) Seed Powder as a Biobased Ingredient for the Production of Cosmetic Products. Cosmetics. 2023;10(3):90.
60. Esho BA, Samuel B, Akinwunmi KF, Oluyemi WM. Membrane stabilization and inhibition of protein denaturation as mechanisms of the anti-inflammatory activity of some plant species. Trends in Pharmaceutical Sciences. 2021;7(4):269-78.
61. Dewanjee D, Ghosh S, Khatua S, Rapior S. Ganoderma in skin health care: A state-of-the-art review. Ganoderma. 2024:79-101.
62. Latreille B, Paquin P. Evaluation of emulsion stability by centrifugation with conductivity measurements. Journal of food science. 1990;55(6):1666-8.
63. EL-OTMANI, Najlae (2025). Phytochemical profiling, enzymes inhibition, anti-inflammatory, antidermatophytes 989 activities_Raw_Data. figshare. Dataset. https://doi.org/10.6084/m9.figshare.28714856.v1